Supplementary Materials

for

Electrospun Cr-doped $Bi_4Ti_3O_{12}/Bi_2Ti_2O_7$ Heterostructures Fibers with Enhanced Visible-Light Photocatalytic Properties

Hongfei Shi,[ab] Huaqiao Tan,[ab]* Wan-bin Zhu, [c] Zaicheng Sun,[a]* Yuejia Ma [a] and Enbo Wang[b]*

[a] State Key Laboratory of Luminescence and Applications, Changchun Institute of Optics, Fine Mechanics and Physics, Chinese Academy of Sciences, 3888 East Nanhu Road, Changchun 130033, People's Republic of China.

[b] Key Laboratory of Polyoxometalate Science of Ministry of Education, Department of Chemistry, Northeast Normal University, Ren Min Street No. 5268, Changchun, Jilin, 130024, People's Republic of China.

[c] State Key Laboratory of Applied Optics, Changchun Institute of Optics, Fine Mechanics and Physics, Chinese Academy of Sciences, Changchun 130033, China

sunzc@ciomp.ac.cn(ZS)

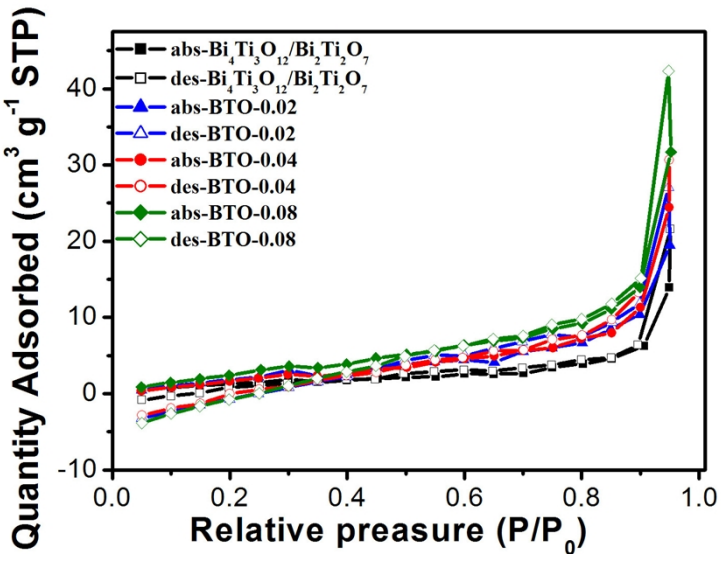

Fig. S1. The nitrogen adsorption-desorption isotherms curves of $Bi_4Ti_3O_{12}/Bi_2Ti_2O_7$, BTO-0.02, BTO-0.04 and BTO-0.08 (abs = adsorption, des = desorption).

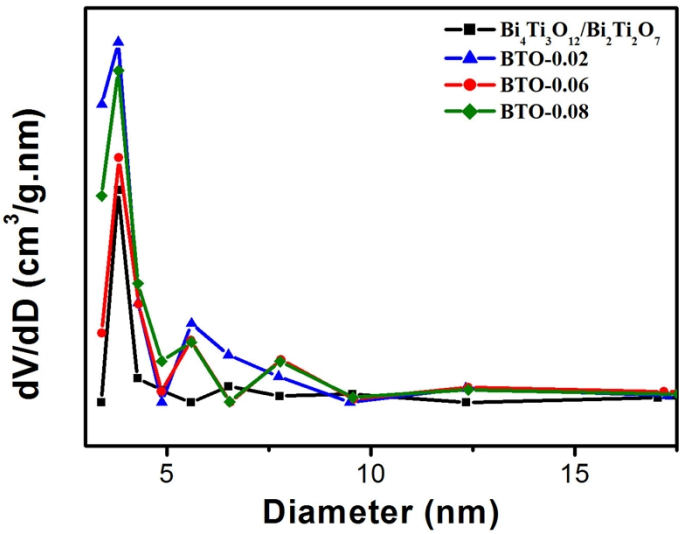

Fig. S2 The pore size distribution curves of $Bi_4Ti_3O_{12}/Bi_2Ti_2O_7$, BTO-0.02, BTO-0.04 and BTO-0.08.

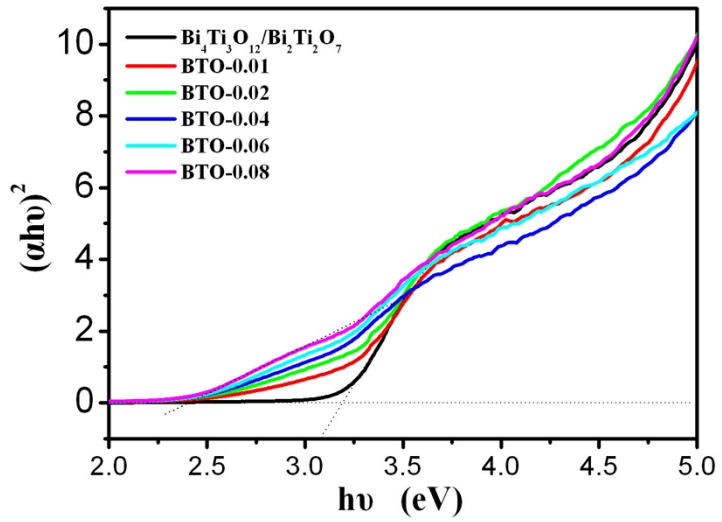

Fig. S3 The band-gap evaluation from the plots of $(\alpha h\upsilon)^2$ vs. $h\upsilon$ of BTO samples.

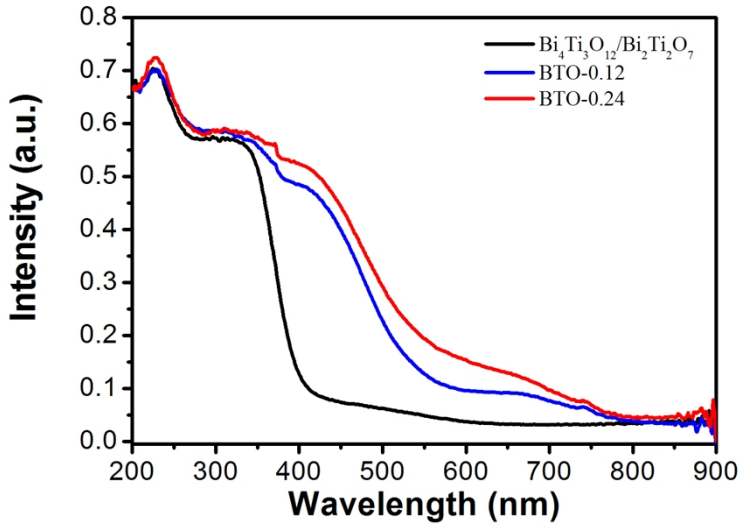

Fig. S4. UV-vis diffuse reflectance spectra of the $Bi_4Ti_3O_{12}/Bi_2Ti_2O_7$ fibers, BTO-0.12 and BTO-0.24.

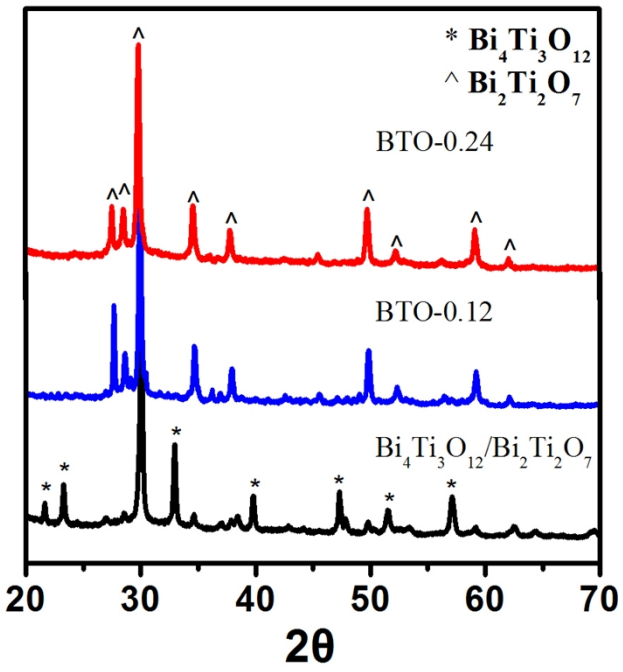

Fig. S5. The XRD of the $Bi_4Ti_3O_{12}/Bi_2Ti_2O_7$ fibers, BTO-0.12 and BTO-0.24.

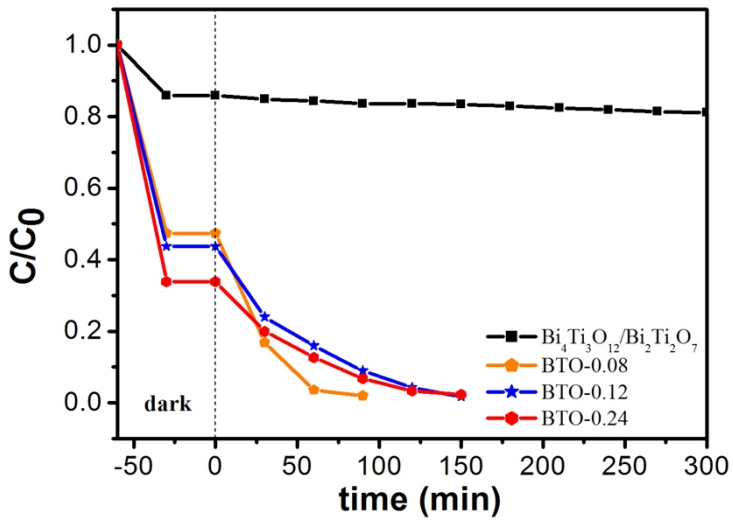

Fig. S6. Degradation profiles of MO, where C is the concentration of the MO, C_0 is the initial concentration of MO.

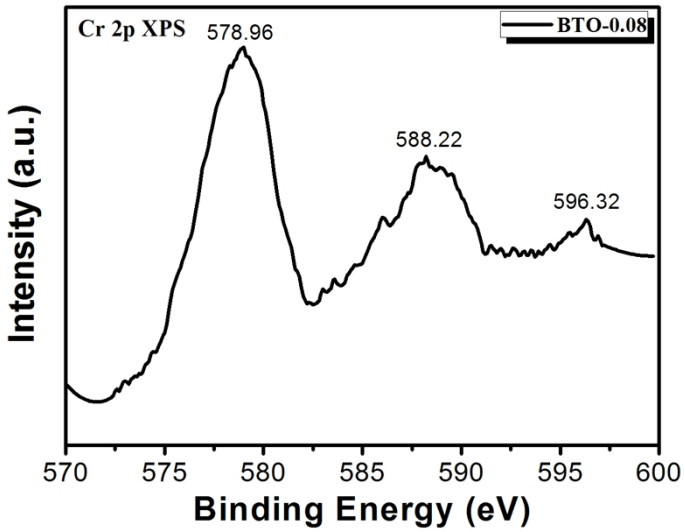

Fig. S7. The Cr 2p XPS spectra of BTO-0.08.

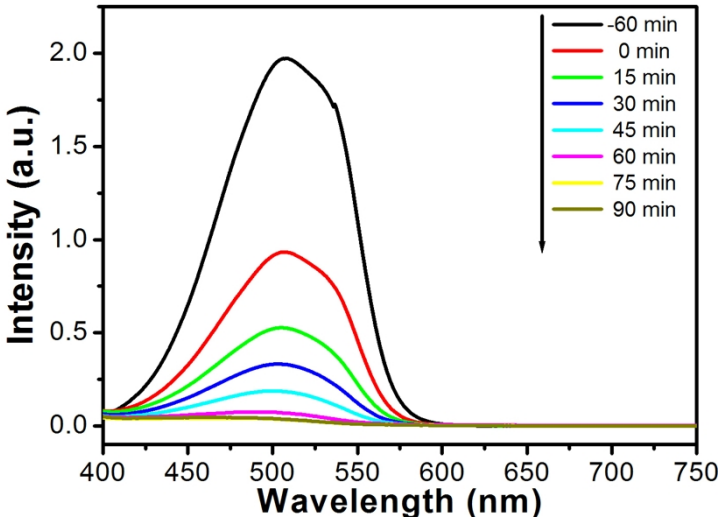

Fig. S8 Degradation of MO using BTO-0.08 as catalyst under visible light irradiation.

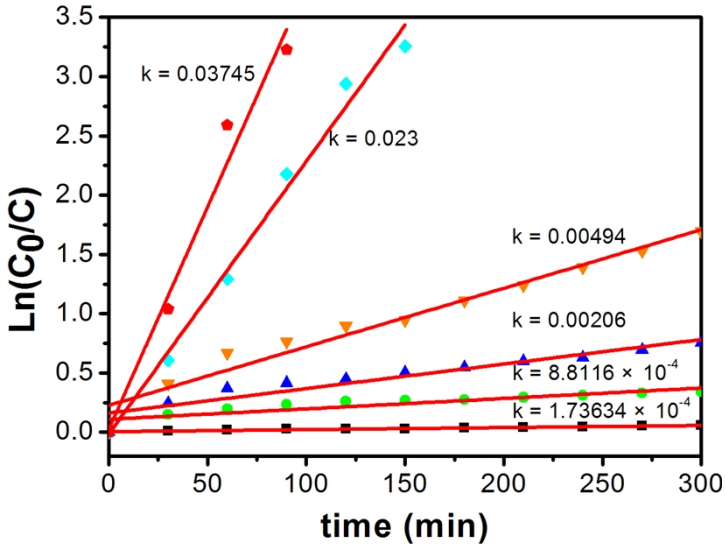

Fig. S9 Kinetic linear simulation curves of MO photocatalytic degradation with the $Bi_4Ti_3O_{12}/Bi_2Ti_2O_7$ and BTO fibers.

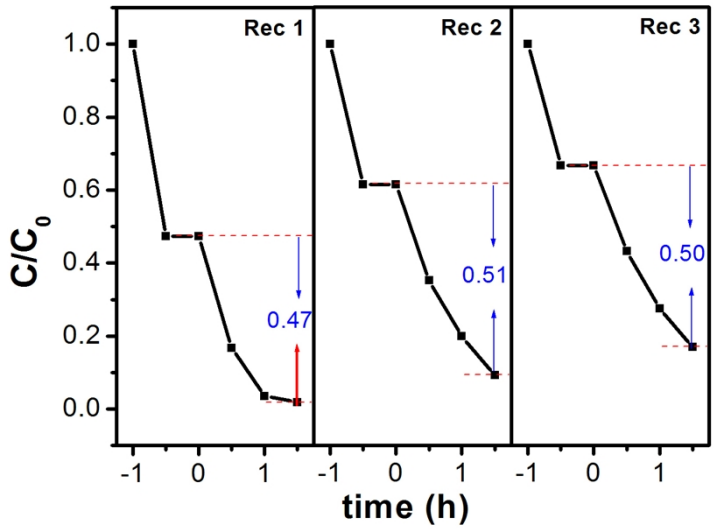

Fig. S10 Cycling runs of photocatalytic degradation of MO in aqueous BTO-0.08 dispersions under visible light irradiation, where C is the concentration of the MO, C_0 is the initial concentration of MO.

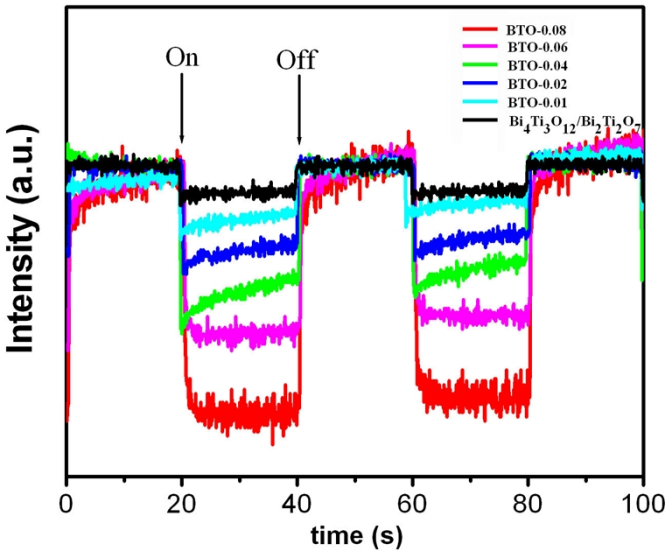

Fig. S11 Transient photocurrent response of $Bi_4Ti_3O_{12}/Bi_2Ti_2O_7$ and BTO samples in 0.5 M Na_2SO_4 aqueous solutions under visible-light irradiation at 0 V *vs*. Hg/Hg_2Cl_2

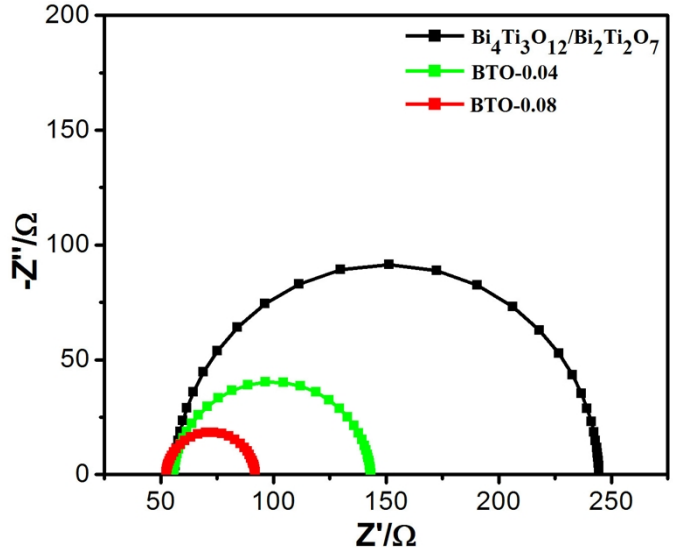

Fig. S12. The electrochemical impedance spectroscopy (EIS) of $Bi_4Ti_3O_{12}/Bi_2Ti_2O_7$, BTO-0.04 and BTO-0.08. Electrochemical impedance spectroscopy (EIS) was performed using a Model CS350 electrochemistry station (CH Instruments, Wuhan CorrTest Instrument Corporation, PRC) in 0.1 M $LiClO_4$ ethanol solution at +0.25 V from 0.1 Hz to 100 KHz . The EIS data were fitted using ZSimpWin data analysis software.